STUDY ON THE EFFECTIVENESS AND SUPPRESSION MECHANISM OF DRY WATER MATERIALS IN INHIBITING H_2/CH_4 EXPLOSIONS IN HORIZONTAL PIPELINES

Song LIN* [*], *Emmanuella Enosa Lomeling ZACHARIA, Yanting CAO,

Lanyun WANG, Yunhao LI* [*], *and Ming PENG

School of Safety Science and Engineering, Changzhou University, Changzhou 213164, China

[*] Corresponding authors; e-mail: LS@cczu.edu.cn; liyunhao@cczu.edu.cn

To investigate the suppression effect of dry water materials on H_2/CH_4 explosions, dry water materials were prepared and explosion suppression experiments were conducted using a self-built long straight steel pipe explosion test apparatus. The results indicate that a certain mass of dry water materials can effectively suppress explosions, reducing both the peak overpressure and peak rate of pressure rise. However, insufficient dry water material actually promotes H_2/CH_4 explosions, while excessive amounts diminish the suppression effect. Under the combined effects of high explosion temperatures and shock waves, the rupture of dry water materials exposes water to the combustion space. This absorbs substantial heat, exerting a cooling effect. Simultaneously, gaseous water dilutes oxygen concentration, inhibiting combustion. As the volume fraction of water participating in combustion increases, although $H+O_2=O+OH$ continues to enhance combustion, the inhibitory effect of $H+CH_3(+M)=CH_4(+M)$ also intensifies. Once water concentration reaches a certain threshold, the promoting effect of $HCO+M=H+CO+M$ disappears, giving way to a new elementary reaction: $H+CH_4=CH_3+H_2$, which inhibits combustion. This research provides valuable reference for preventing and controlling H_2/CH_4 explosions.

Keywords*: dry water materials, gas explosion, hydrogen energy safety, explosion suppression*

1. Introduction

Explosions caused by flammable gases occur frequently, hindering the adoption of new clean energy sources such as hydrogen gas [1,2]. Therefore, there is an urgent need to develop and optimize safety protection technologies to prevent accidents and mitigate their consequences. Powdered explosion-suppression materials have garnered widespread attention due to their high efficiency, cost-effectiveness, environmental friendliness, stable performance, and long service life [3,4].

Dry water (DW) material is a white powder produced by fragmenting deionized water into fine droplets via high-speed dispersion and coating them with hydrophobic SiO_2. Its primary component is water, conferring advantages of abundant raw materials, low cost, and a simple, non-polluting production process, which makes it an environmentally friendly material [5]. With a water content exceeding 90% by mass, DW material serves as an excellent fire extinguishing agent. It can effectively suppress oil fires [6,7], lithium battery thermal runaway fires [8], coal spontaneous combustion [9], and wood fires [10].

In recent years, researchers have progressively applied DW materials to suppress gas and dust explosions. Wang *et al*. [11] and Jiang *et al*. [12] investigated the suppression effects of DW materials on polypropylene dust explosions and coal dust explosions using a 20 L spherical explosion apparatus, respectively. The results indicate that DW materials can suppress dust explosions to a certain extent. Chen *et al*. [13] tested the suppression effect of DW materials on methane explosion using a near-spherical explosion device with a volume of 20 L. Wang *et al*. [14] employed $NH_4H_2PO_4$ modified DW materials to suppress methane explosions. Results demonstrated that compared to unmodified DW, the modified DW materials exhibited both physical and chemical suppression effects, significantly enhancing the suppression efficacy. Wang *et al*. [15] incorporated gelling agents during the preparation of modified DW materials, resulting in enhanced suppression efficiency of the synthesized modified calcium alginate DW materials and relatively stable particle structure. Peng *et al*. [16] investigated the effects of calcium alginate gel and urea modified DW materials on the radical spectral characteristics and suppression mechanisms in methane explosions, achieving reductions in maximum explosion pressure ranging from 39.24% to 76.95%. Yang *et al*. [17] found that sodium salt modified DW materials inhibits methane explosions through both physical and chemical suppression mechanisms. Zeng *et al*. [18] investigated the explosion suppressing effects of DW materials prepared with super absorbent polymers (SAP) and ammonium polyphosphate as additives. Their findings revealed that incorporating SAP significantly enhanced the stability and water retention capacity, while also improving its chemical explosion-suppression efficacy. Gao *et al*. [19] investigated the synergistic suppression of methane explosions by flame-retardant modified DW materials, discovering that its unique core-shell structure endows it with explosion-inhibiting properties capable of exerting both solid-phase and liquid-phase suppression effects simultaneously. Qiu *et al*. [20] examined the characteristics of bio-based modified DW materials in suppressing methane explosions, providing a green framework for designing novel gel DW materials.

Current research primarily focuses on the fire extinguishing performance and mechanisms of DW materials, as well as their suppression effects on methane explosions. The combustion of hydrogen-methane mixtures reduces CO_2 emissions and is a key hydrogen energy direction, but explosion prevention remains a major research focus [21-23]. It is worthwhile to investigate the effectiveness and suppression mechanisms of DW materials in H_2/CH_4 explosions. Therefore, this paper employs a self-built long straight pipe explosion test system to investigate the influence of DW materials on the peak overpressure and peak rate of pressure rise in H_2/CH_4 explosions. The mechanism by which the DW material inhibits H_2/CH_4 explosion was investigated using a combination of scanning electron microscopy (SEM), TG-DSC, and Chemkin simulations. The findings provide valuable reference for developing powdered explosion suppressants to prevent hydrogen-containing gas explosions.

2. Experimental and simulation methods

2.1. Explosion test apparatus

The explosion tests were conducted at room temperature using a self-built explosion test apparatus. The explosion test apparatus primarily consists of a pipeline, a gas distribution system, an ignition system, and an explosion overpressure data acquisition system, as shown in Figure 1. The H_2/CH_4 explosion experiment was conducted in a steel pipe measuring 1800 mm in length and 100 mm in inner diameter. The pipeline can withstand a pressure of up to 2.0 MPa. The ignition system employed an igniter mounted on the blind flange on the left side of the pipe to achieve electric spark discharge ignition. Gas distribution was based on Dalton's law of partial pressures. The data acquisition system comprised a pressure sensor, charge adapter, and multi-channel data acquisition unit. Six pressure sensors mounted on the pipe wall collected explosion pressure signals at positions corresponding to length-to-diameter ratios of 1.5, 4.5, 7.5, 10.5, 13.5, and 16.5. The pressure sensors had a measurement range of 0–1.0 MPa.

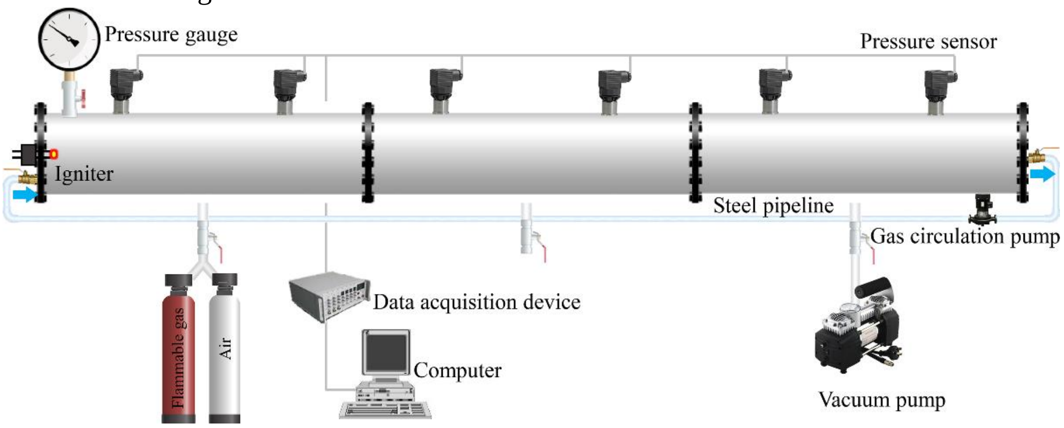

Figure 1. Explosion test apparatus

2.2. Experiments materials

With a hydrogen blending ratio of up to 20%, end-use devices such as residential gas stoves, water heaters, and industrial boilers can operate stably without requiring major modifications. Therefore, methane with a 20% hydrogen blending ratio was selected for testing in this work. The flammable gas mixture is supplied by Changzhou Dacheng Gas Co., Ltd. The materials required for the preparation of dry water are deionized water and nanoscale hydrophobic silica. Deionized water was produced in the laboratory by removing ionic substances and impurities from the water. Hydrophobic nano-silica was supplied by Shaoxing Lijie Chemical Co., Ltd. Through testing under various parameters, the preparation process for DW materials was determined, yielding optimal ratios, stirring speeds, and stirring times. As shown in Figure 2, the DW materials was prepared using nano-silica and deionized water at a mass ratio of 1:13, stirred at 11,000 rpm for 5 seconds, with these parameters determined based on our previous work [22].

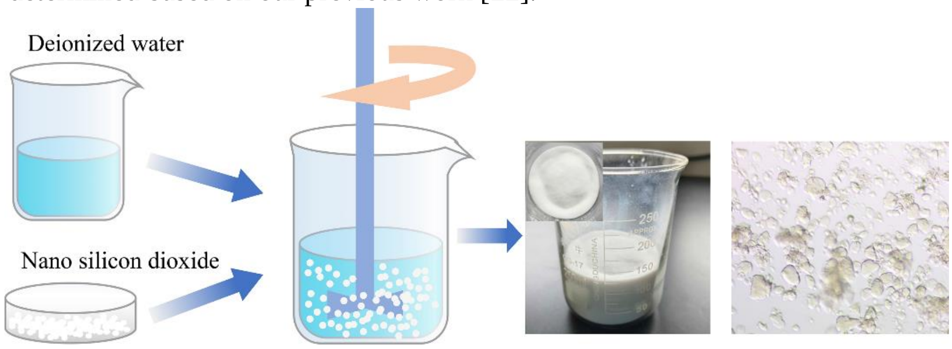

Figure 2. DW materials preparation process

The particle size distribution of the prepared DW material is shown in Figure 3. In addition, the characteristics of the DW material were evaluated by measuring its bulk density, water retention, and angle of repose. Bulk density refers to the density of powder after natural accumulation without compaction, defined as the ratio of the powder's mass to the volume it occupies in the container. The average bulk density of the prepared DW materials was 0.427 g·ml^{-1}. Water retention capacity is a key indicator for evaluating the quality and stability of DW material. After a 12-hour treatment at 30 °C, the prepared DW material exhibited a water retention rate of 89.35%. The angle of repose denotes the maximum angle formed between the free surface of a static powder layer and the horizontal plane, exhibiting an inverse relationship with the powder's flowability. The prepared DW material exhibited an angle of repose of 26.34°. The microstructure of the DW material was observed using scanning electron microscopy. As shown in Figure 4, the prepared DW material exhibits a stable core-shell structure with water as the core and silica as the shell.

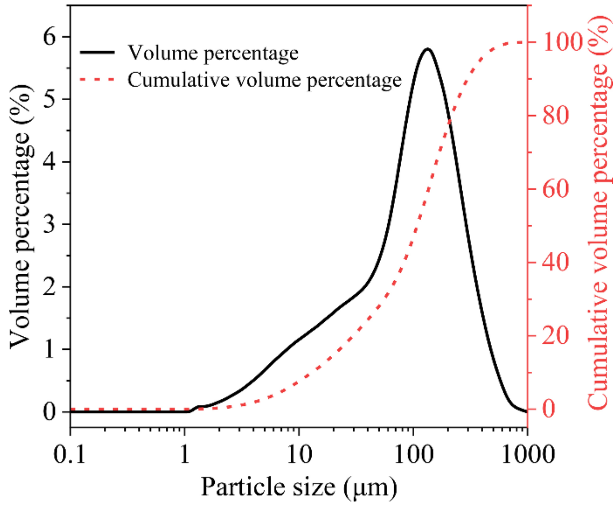

Figure 3. Particle size distribution of the prepared DW materials

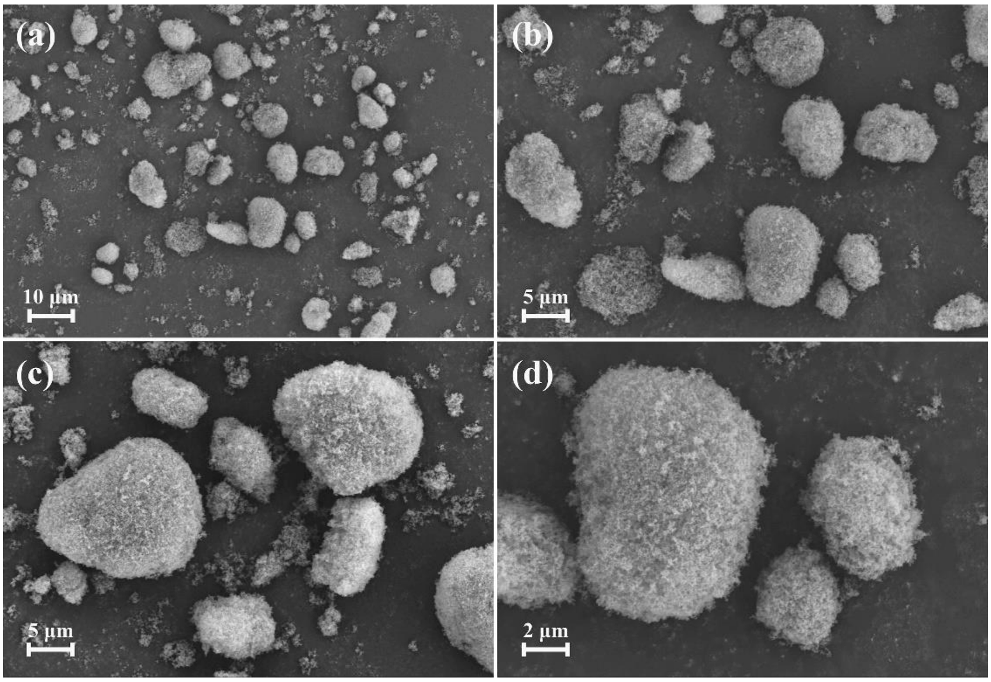

Figure 4. SEM images of the prepared DW materials

2.3. Analysis methods for suppression mechanisms

(1) SEM observation.

The microstructure of DW materials before and after the H_2/CH_4 explosion was observed using scanning electron microscopy to infer its role during the explosion process.

(2) TG-DSC analysis.

The weight loss and endothermic characteristics of DW materials under high-temperature conditions were investigated through TG-DSC. The thermal testing was conducted under controlled conditions with a heating rate of 10 K/min in an air atmosphere.

(3) Chemkin methord.

Using Chemkin software and the premixed laminar flame model, chemical kinetics simulations were conducted for laminar burning of H_2/CH_4 with added water. The widely used GRI 3.0 mechanism, whose accuracy has been validated in laminar combustion simulations of H_2/CH_4 mixtures [23], was therefore also adopted in this study. The unburned gas temperature was set to 298 K, with atmospheric pressure at 1 atm. The maximum allowed grid count was set to 4000, with grid gradient and curvature set to 0.1 and 0.5 respectively. The computational domain extended from 0 to 1.0 cm. Thermal diffusion effects were incorporated in the calculations. For species transport, the multi-component mixed-average transport method was selected. Both convective and diffusive terms employed upwind differencing. The computational control equations primarily include the mass conservation equation, energy conservation equation, component transport equations, and ideal gas state equation [24], which are respectively:

$$M = \rho u A \tag{1}$$

$$M\frac{\mathrm{d}T}{\mathrm{d}x}-\frac{1}{c_\mathrm{p}}\frac{\mathrm{d}}{\mathrm{d}x}\left(\lambda A\frac{\mathrm{d}T}{\mathrm{d}x}\right)+\frac{A}{c_\mathrm{p}}\sum_{k=1}^{n}\rho Y_k c_{\mathrm{p}k}\frac{\mathrm{d}T}{\mathrm{d}x}+\frac{A}{c_\mathrm{p}}\sum_{k=1}^{n}\omega_k h_k W_k=0 \tag{2}$$

$$M\frac{\mathrm{d}Y_k}{\mathrm{d}x}+\frac{\mathrm{d}}{\mathrm{d}x}(\rho A Y_k V_k)-A\omega_k W_k=0 \tag{3}$$

$$\rho RT = PW_\mathrm{A} \tag{4}$$

where M is the mass flow rate, ρ – the gas density, u – the gas flow velocity, A – the cross-sectional area, T – the temperature, x – the axial coordinate, c_p – the specific heat capacity at constant pressure for the mixture, $c_{\mathrm{p}k}$ – the specific heat capacity at constant pressure for the kth gas, λ – the thermal conductivity, Y_k – the mass fraction of the kth gas, V_k – the diffusion rate of the kth gas, ω_k – the reaction production rate of the kth gas, h_k – the specific enthalpy of the kth gas, W_k – the molecular weight of the kth gas, R – the gas constant, P – the pressure, W_A – the average molecular weight.

3. Results and discussion

3.1. Explosion characteristics of H_2/CH_4 in the pipeline

Typical explosion pressure recording curves are shown in Figure 5. After ignition, the explosion overpressure at the measurement point rapidly rises and then falls. The rate of pressure rise initially increases, then decreases to a negative value before stabilizing at zero. During each test, the maximum pressure signal recorded at the measurement point represents the overpressure peak. The rate of pressure rise is obtained through differentiation, with its maximum value representing the peak rate of pressure rise. To characterize H_2/CH_4 explosions under different operating conditions, the peak overpressure and peak rate of pressure rise are extracted for analysis.

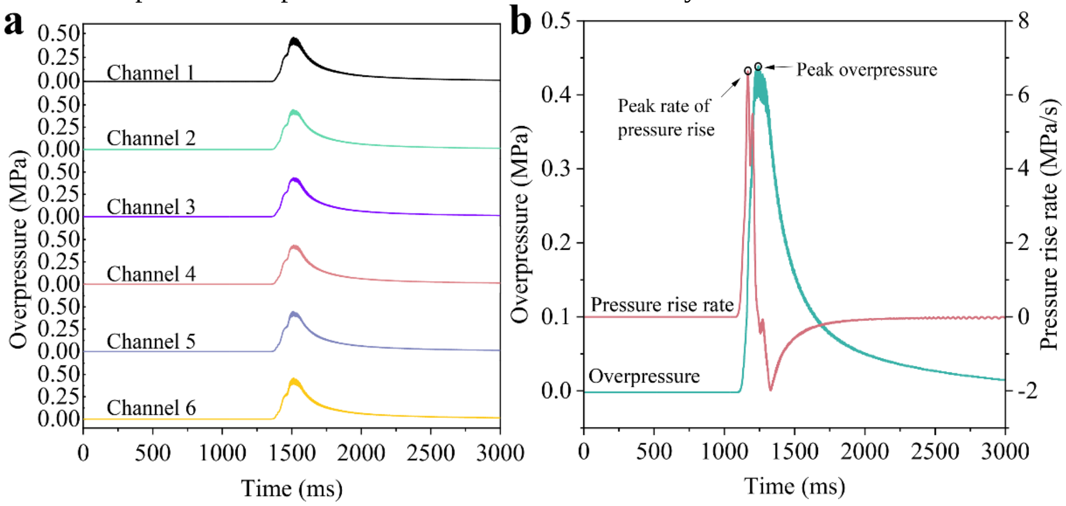

Figure 5. Typical explosion pressure curves

Figure 6 displays the peak overpressure and peak rate of pressure rise for H_2/CH_4 (contains 20% H_2) explosions. It is evident that variations in the equivalence ratio significantly influence both the peak overpressure and peak pressure rise rate. As the length-to-diameter ratio increases, both the peak overpressure and peak rate of pressure rise fluctuate, though the magnitude of change is modest. It can be observed that with increasing equivalent ratio, the peak overpressure and peak rate of pressure rise of H_2/CH_4 first increase and then decrease. At an equivalent ratio of 1.2, both values reach their maximum. Generally, the peak overpressure of flammable gas explosions exhibits a trend of first increasing and then decreasing with rising equivalence ratio. At an equivalence ratio slightly above 1.0, the maximum explosion pressure is reached [25, 26]. This demonstrates that the experimental results in this paper are consistent with theoretical predictions, thereby confirming the reliability of the experimental findings.

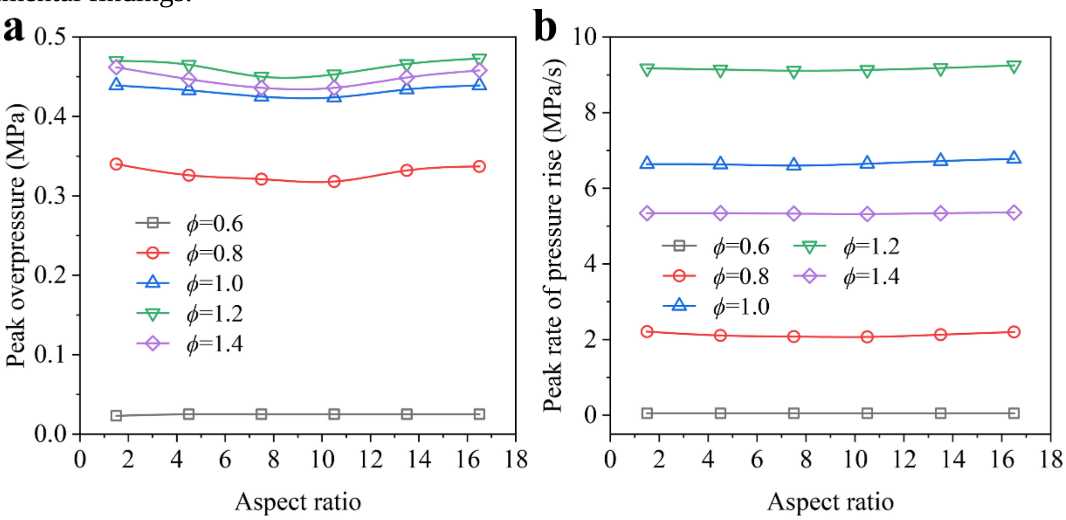

Figure 6. Peak overpressure and peak rate of pressure rise of H_2/CH_4 explosions

3.2. Effect of DW materials on the explosion characteristics of H_2/CH_4 mixtures

Drawing from the above results, the effect of the DW material, which was evenly laid in the first pipe, on a H_2/CH_4 explosion at an equivalence ratio of 1.2 was tested. The application of DW material inside the pipe produces a systematic effect on the characteristics of H_2/CH_4 explosions, as shown in Figure 7. It should be noted that when the DW material application amount is 2g, both the peak overpressure and peak rate of pressure rise increase. The primary reason for promoting explosions with smaller amounts of DW material is the increased number of active free radicals resulting from water molecule decomposition at high temperatures, coupled with potential flame turbulence caused by the rupture of the DW material [13]. As the amount of DW material increases beyond 4 g, the explosions are effectively suppressed, a phenomenon observable at different aspect ratios. At a DW mass of 6 g, the peak overpressure of decreased to a minimum of 0.40 MPa, while the peak rate of pressure rise decreased to 3.45 MPa/s. However, the explosion suppression effect weakened at a DW mass of 8 g. A possible explanation for this observation is the sedimentation and agglomeration of the DW material [27]. As the material settles and forms larger aggregates, its effective surface area diminishes, which in turn impairs the thermal decomposition efficiency.

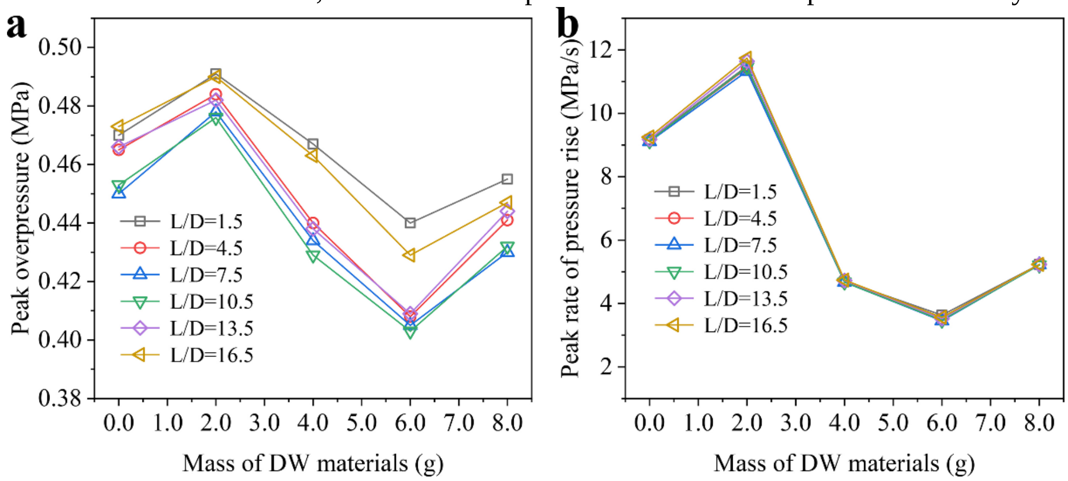

Figure 7. Explosion peak overpressure and peak rate of pressure rise for H_2/CH_4 varying with DW material mass

Figure 8 shows the variation in the peak overpressure and peak rate of pressure rise of H_2/CH_4 explosions when DW material is incorporated, as a function of the aspect ratio. It can be observed that when sufficient DW material participates in the explosion, a significant reduction in peak overpressure occurs near the DW material placement location (at an aspect ratio of 4.5), demonstrating the effective explosion suppression characteristics of the DW material. However, a pressure increase trend appears near the pipeline end, resulting from pressure accumulation at the closed terminal.

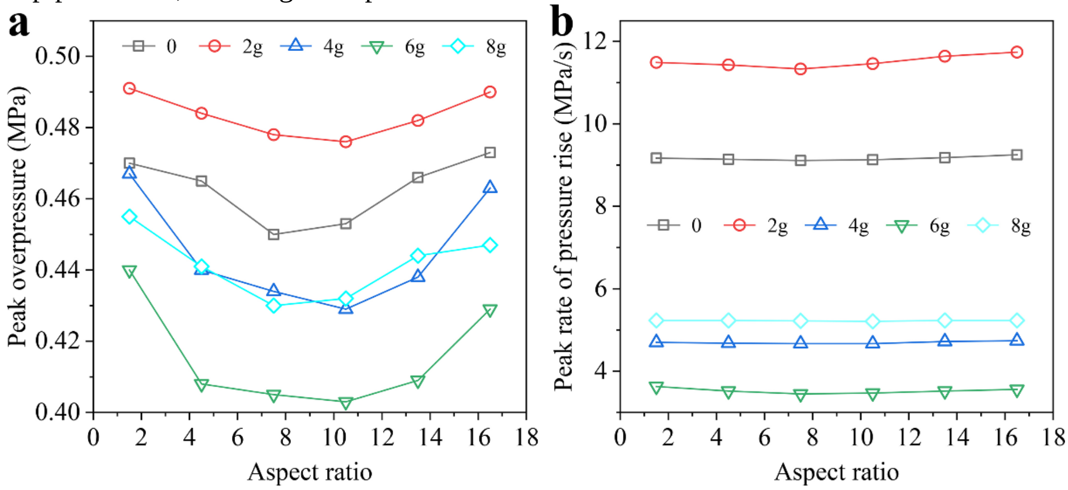

Figure 8. The peak overpressure and peak rate of pressure rise in H_2/CH_4 explosions influenced by DW materials varying with the aspect ratio

3.3. Analysis of the suppression mechanism of DW materials in H_2/CH_4 explosions

The structure of DW material is characterized by nano-silica encapsulating a large volume of deionized water. During gas explosions, nano-silica acts as a physical barrier. Additionally, water plays a crucial role in suppressing explosions after the core-shell structure of DW materials is disrupted by explosion shock waves and high temperatures. Residual DW materials after suppressing the hydrogen-methane explosion were collected and examined using an electron scanning microscope. The microstructure of the residual DW materials is shown in Figure 9, revealing that the core-shell structure of the DW materials was indeed destroyed by the explosion shock waves and high temperatures.

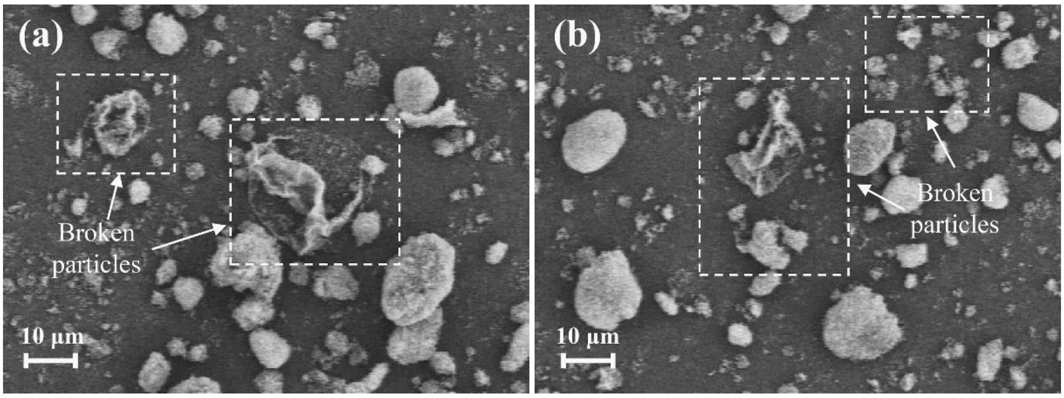

Figure 9. Microstructure of the DW material after explosion

DW materials may adversely affect the suppression of hydrogen-methane mixture explosions due to either insufficient or excessive quantities drawn into the explosion reaction zone. However, this paper will not further explore this cause, which has already been briefly discussed in the preceding section. Below, the focus will shift to analyzing how water within DW materials suppresses hydrogen-methane mixture explosions. Figure 10 shows the thermogravimetric and endothermic characteristics of the prepared DW material under an air atmosphere at a heating rate of 10 K/min. The prepared DW material exhibits a single-stage thermogravimetric feature. The weight loss process is completed at approximately 130 °C, with a maximum weight loss rate of 19.44 %/min reaching at 109.56 °C. This stage is caused by the loss of water from the prepared DW material. A significant endothermic peak can be observed during this stage, with an endothermic power of up to 10.55 W/g at 115.77 °C. This indicates that the water in the prepared DW material can effectively mitigate H_2/CH_4 explosion reactions through heat absorption.

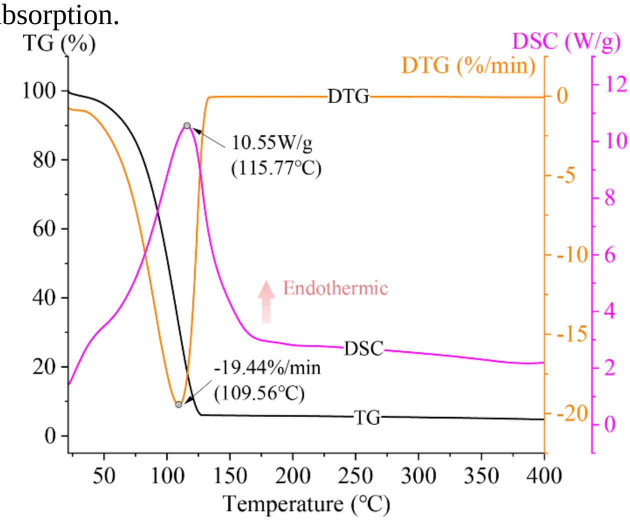

Figure 10. TG-DSC analysis of the prepared DW material

Figure 11 illustrates the influence of water vapor on the laminar burning velocity and maximum flame temperature of the mixture consist of 20%H_2 and 80%CH_4 at an equivalence ratio of 1.2. It can be observed that the volume fraction of water vapor participating in the reaction exhibits a largely linear negative correlation with both the laminar burning velocity and the maximum flame temperature.

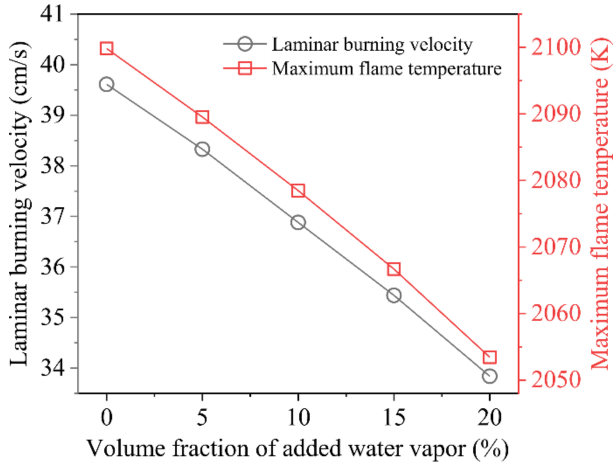

Figure 11. The effect of water vapor on laminar burning velocity and maximum flame temperature

The effect of water vapor on heat production during H_2/CH_4 premixed combustion is shown in Figure 12. As the volume fraction of water vapor participating in the reaction increases, the heat production during combustion gradually decreases. It can be inferred that under the combined effects of explosion high temperatures and shock waves, the rupture of DW material allows water to interact with the combustion space, absorbing substantial heat and thereby exerting a cooling effect.

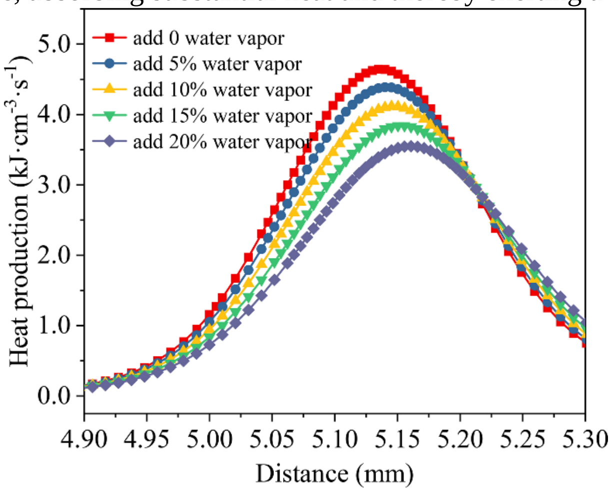

Figure 12. The effect of water vapor on heat production

Beyond physical effects, water can participate in combustion reactions, chemically inhibiting the combustion of H_2/CH_4. Elementary reaction analysis provides insights into the chemical mechanisms underlying premixed combustion at the microscopic level [28]. As shown in Figure 13 and Table 1, the most significant key elementary reaction promoting laminar combustion of H_2/CH_4 is $H+O_2=O+OH$, while the most significant key elementary reaction inhibiting laminar combustion is $H+CH_3(+M)=CH_4(+M)$. As the volume fraction of water vapor participating in combustion increases, although $H+O_2=O+OH$ continues to enhance combustion promotion, the inhibitory effect of $H+CH_3(+M)=CH_4(+M)$ also intensifies. Furthermore, when water content reaches 10% and above, the promoting effect of HCO+M=H+CO+M disappears, and a new elementary reaction $H+CH_4=CH_3+H_2$ emerges to inhibit combustion.

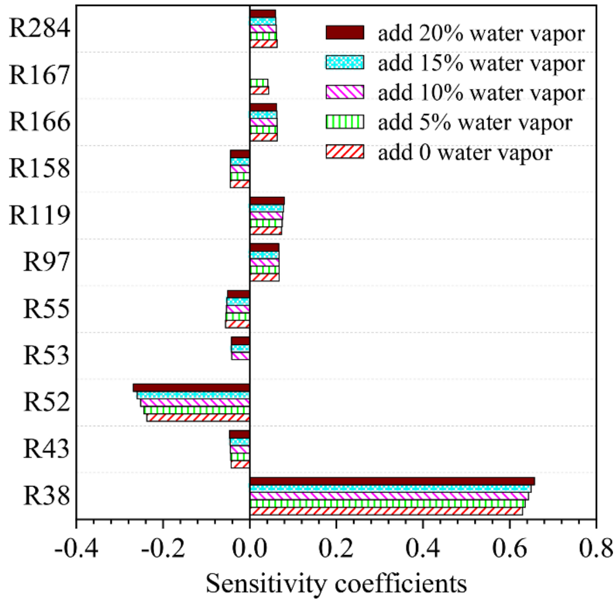

Figure 13. Sensitivity analysis

Table 1. The primary elementary reactions involved

Serial number	Reaction number	Elementary reaction
1	R38	$H+O_2=O+OH$
2	R43	$H+OH+M=H_2O+M$
3	R52	$H+CH_3(+M)=CH_4(+M)$
4	R53	$H+CH_4=CH_3+H_2$
5	R55	$H+HCO=H_2+CO$
6	R97	$OH+CH_3=CH_2(S)+H_2O$
7	R119	$HO_2+CH_3=OH+CH_3O$
8	R158	$2CH_3(+M)=C_2H_6(+M)$
9	R166	$HCO+H_2O=H+CO+H_2O$
10	R167	HCO+M=H+CO+M
11	R284	$O+CH_3=H+H_2+CO$

4. Conclusion

In this study, DW materials were prepared, and their suppression effect on H_2/CH_4 explosions was investigated using a horizontal long straight pipe explosion test apparatus. The influence of water, the primary component in DW materials, on the chemical kinetics of H_2/CH_4 premixed combustion was analyzed using Chemkin software. Results indicate that sufficient DW materials effectively suppresses explosions by reducing peak overpressure and peak rate of pressure rise. However, excessive DW materials diminishes suppression efficacy. Notably, insufficient DW materials mass actually increases the peak overpressure and peak rate of pressure rise of H_2/CH_4 explosions. DW materials suppress H_2/CH_4 explosions through both physical and chemical mechanisms. Water within the material absorbs substantial heat generated by the explosion, providing a cooling effect, while gaseous water dilutes oxygen concentration, weakening the explosive reaction. As the volume fraction of water vapor participating in combustion increases, although $H+O_2=O+OH$ continues to enhance combustion, the inhibitory effect of $H+CH_3(+M)=CH_4(+M)$ also intensifies. Upon reaching a certain water concentration, the promoting effect of HCO+M=H+CO+M disappears, giving way to a new elementary reaction: $H+CH_4=CH_3+H_2$, which suppresses combustion. DW material is both eco-friendly and cost-effective, rendering it a very promising candidate for explosion suppression. Nevertheless, the present investigation was carried out solely under laboratory pipeline conditions. For real industrial applications, the effects of various parameters such as spatial dimensions and obstacles require further consideration.

Acknowledgment

The authors acknowledge support from the National Natural Science Foundation of China (Grant Nos. 52304205 and 52474206).

References

[1] Zhou, G., *et al*., Study on explosion dynamics and kinetic mechanism of DME/H_2 blended gas at typical fuel-lean/rich concentrations, *Case Studies in Thermal Engineering*, *40* (2022), 102444

[2] Zhang, X., *et al*., Effects of hydrogen addition on methane explosion behaviors and microscopic mechanism within a confined system, *International Journal of Hydrogen Energy*, *198* (2026), 152782

[3] Wang, W., *et al*., Explosion suppression characteristics of ferrocene–silica composite powders in hydrogen explosions, *Combustion and Flame*, *285* (2026), 114712

[4] Hua, M., *et al*., Experimental study on the suppression effect of composite ultrafine dry powder fire extinguishing agents containing ternary layered double hydroxides on hydrogen deflagration, *Chemical Engineering Journal*, *526* (2025), 171140

[5] Saleh, K., *et al*., Dry water: From physico-chemical aspects to process-related parameters. *Chemical Engineering Research and Design*, *89* (2011), 5, pp. 537–544

[6] Wang, L., *et al*., Enhanced fire-extinguishing performance of struvite powder through modulation of its thermal-decomposition characteristics, *Fire Safety Journal*, *159* (2026), 104594

[7] Ding, W., *et al*., Performance and fire suppression efficiency of potassium salt-modified dry water agents, *Journal of Loss Prevention in the Process Industries*, *100* (2026), 105869

[8] Chai, G., *et al*., Experimental study on dry water inhibiting thermal runaway of ternary lithium-ion battery, *Journal of Thermal Analysis and Calorimetry*, *150* (2025), 19, pp. 14959–14972

[9] Dou, G., *et al*., Lignin-Based Hydrogel Reinforced Dry Water as Inhibitor for Coal Spontaneous Combustion, *Combustion Science and Technology*, *196* (2024), 17, pp. 4391–4409

[10] Chai, G., *et al*., Experimental study on the effect of dry water materials on the fire extinguishing efficiency and suppression mechanism of wood crib fire, *Fire and Materials*, *48* (2024), 4, pp. 469–482

[11] Wang, J., *et al*., Effect of modified dry water on the explosion characteristics of polypropylene dust, *Powder Technology*, *469* (2026), 121936

[12] Jiang, B., *et al*., Synthesis of modified dry water explosive suppressant and its suppression of coal dust explosion characteristics research, *Powder Technology*, *469* (2026), 121814

[13] Chen, X., *et al*., Experimental study on suppression of gas deflagration by dry water materials, *Explosion and Shock Waves*, *39* (2019), 11, pp. 120–130

[14] Wang, Q., *et al*., Gas explosion suppression by ammonium dihydrogen phosphate-modified dry water powder, *Powder Technology*, *416* (2023), 118228

[15] Wang, Q., *et al*., Gas explosion suppression performance of modified gel-type dry waters, *Powder Technology*, *420* (2023), 118378

[16] Peng, B., *et al*., Impact of calcium alginate gel-urea modified dry water on free radical spectral signatures and suppression mechanisms in methane explosions, *Process Safety and Environmental Protection*, *202* (2025), 107733

[17] Yang, Z., *et al*., The deflagration suppression of methane-air by sodium salt-modified dry water: Experimental and kinetic investigation, *Journal of Loss Prevention in the Process Industries*, *98* (2025), 105743

[18] Zeng, H., *et al*., A novel gel dry water: preparation and application in methane-air explosion, *Process Safety and Environmental Protection*, *186* (2024), June, pp. 134–150

[19] Gao, J., *et al*., Investigation on the synergistic suppression effect of flame retardant-modified dry water on methane explosion, *Powder Technology*, *454* (2025), 120728

[20] Qiu, D., *et al*., Experimental exploration on the suppression of methane-air mixture explosions by bio-based modified gel dry water materials, *Thermal Science and Engineering Progress*, *60* (2025), 103387

[21] Luo, Z., *et al*., Experimental study on the explosion inhibition of H_2/CH_4/air mixture using modified $KHCO_3$, *International Journal of Hydrogen Energy*, *145* (2025), July, pp. 1007–1018

[22] Zhang, H., *et al*., The availability of industrial purge gas: Experimental and kinetic study of explosion characteristics of low-concentration H_2/CH_4 mixtures, *Energy*, 313 (2024), 133910

[23] Duan, Y., *et al*., Study on the protection of flexible facilities in urban underground space against hydrogen-blended methane explosion, *Case Studies in Thermal Engineering*, 73 (2025), 106640

[24] Zhang, Y., *et al*., Experimental study on the effectiveness of new core–shell structure extinguishant to extinguish oil pool fire and analysis of fire extinguishing mechanism, *Journal of Thermal Analysis and Calorimetry*, *150* (2025), 5, pp. 3267–3282

[25] Shang, R., *et al*., Laminar flame speed of H_2/CH_4/air mixtures with CO_2 and N_2 dilution, *International Journal of Hydrogen Energy*, *47* (2022), 75, pp. 32315–32329

[26] Liang, K., Numerical study of water effects on the laminar burning velocity of methanol, *Biomass and Bioenergy*, *108* (2018), Jan., pp. 307–311

[27] Ma, Y., *et al*., Influence of blockage ratio and length-to-diameter ratio on explosion dynamics of DME/H_2 blended gas in semi-open space, *Energy*, *326* (2025), 136258

[28] Liu, Y., *et al*., Experimental study on explosion characteristics of hydrogen–propane mixtures, *International Journal of Hydrogen Energy*, *44* (2019), 40, pp. 22712–22718

[29] Tian, S., *et al*., Suppressive effects of alkali metal salt modified dry water material on methane-air explosion, Energy, 285 (2023), 129547

[30] Wang, Y., *et al*., Effect of concentration on the explosive reaction and mechanism of petroleum ether, *Thermal Science and Engineering Progress*, *64* (2025), 103773

Submitted: 23.01.2026.

Revised: 12.04.2026.

Accepted: 16.04.2026.